Vision Research Vol. 20, pp. 613 to 624
Pergamon Press Ltd 1980. Printed in Great Britain

A FIELD-ADDITIVE PATHWAY DETECTS BRIEF-DURATION, LONG-WAVELENGTH INCREMENTAL FLASHES

BRIAN A. WANDELL* and E. N. PUGH JR
Psychology Department, The University of Pennsylvania, Philadelphia, PA 19174, U.S.A.

(*Received* 13 *August* 1979)

Abstract—This paper reports tests of the hypothesis that a 10 msec, 667 nm, foveal test flash, presented upon a steady, 8° background, is detected by a pathway whose sensitivity is monotonically related to a linear functional of photoreceptor quantum catch. The hypothesis is tested by (1) measuring increment-threshold curves for various background wavelenghts, and (2) measuring threshold upon mixtures of two backgrounds with different wavelengths.

The data are consistent, within measurement error, with the hypothesis. We argue, on grounds of plausibility, that the pathway's sensitivity to the 10 msec test flash is controlled not by an arbitrary linear functional, but by the quantum catch of a single class of photoreceptors.

INTRODUCTION

Among the few hypotheses that all color vision theorists now accept is this: photopic visual function is initiated with photon absorption by the three distinct photopigments of the cone photoreceptors. This hypothesis places an important constraint on color theories: the pigment absorptions are defined as the initial codes of color vision. Thus, the theoretical goal of color science—to provide a rigorous and comprehensive account of color discrimination data—must include a description of the relationship between these fundamental codes and the empirical measurements. Some of the best known examples of comprehensive color vision theories are those of Helmholtz (1896), Schrodinger (1920), and Hurvich and Jameson (1955).

Among the empirical discrimination functions for which a comprehensive theory must give an account are those obtained in two-color increment-threshold experiments (Stiles, 1939, 1953, 1959). Indeed, not long after the initial two-color threshold data were reported, Stiles (1946) himself proposed a line-element theory to explain the basic facts of color discrimination. This theory supposed that the increment threshold results of the 1939 paper directly revealed the spectral sensitivities of the fundamentals. When further empirical observations (Stiles, 1953) showed that the two-color increment thresholds were more complex than they appeared initially, the interpretation of the data was modified. The simple explanation in terms of three cone fundamentals gave way to a more operational theory based on the π-mechanism constructs. These constructs became the primitive objects of the new theory. Their relationship to the fundamentals was left an open problem (Stiles 1967, 1978).

We hope to show that the phenomena we report in this and the following paper (this issue, p. 625) develop our theoretical understanding of the relationship between the π-mechanisms and the three fundamentals of color vision. In these papers we extend the set of two-color increment threshold measurements for a long-wavelength test in two ways. First, by using bi-chromatic fields ranging over a very wide range of intensities, our observations map two-color increment-threshold discriminations in uncharted regions of tristimulus space. Second, by using a 10 msec incremental flash as well as the usual 200 msec flash, we obtain a more comprehensive view of the effects of these fields. These extensions of Stiles' (1939, 1953, 1959) and of Sigel and Pugh's (1980) experiments yield several novel phenomena.

The experiments we report are tests of the consequences of two hypotheses. The first hypothesis is the Principle of Univariance (Naka and Rushton, 1966). This principle asserts that any photoreceptor can signal only the rate at which it is absorbing photons. It cannot signal the wavelength, direction of polarization, or any other property of the absorbed photons (see Rodieck, 1973, p. 262).

The second hypothesis we assume is that threshold for a monochromatic test flash (of an appropriately selected wavelength—here, 667 nm) presented upon a steady adapting field depends only on the number of quanta caught per second from the field by the photopigment of a single class of photoreceptors. We shall refer to this latter hypothesis as the *field quantum-catch hypothesis*, or briefly as the *quantum-catch hypothesis*. This second hypothesis is a psychophysical linking hypothesis.

Our experimental analyses concentrate on two consequences of the above hypotheses. The first is the prediction that the shape of the increment threshold function must not depend on the adapting field wave-

* Present address: Psychology department, Stanford University, Stanford, CA 94305, U.S.A.

length. Stiles calls this property the Field Displacement Law (see, for example, Enoch, 1972).

A second and powerful consequence of the Principle of Univariance and the field quantum-catch hypothesis is this: threshold upon any mixture of two fields is completely determined once the sensitivity to the individual component fields is known. This prediction was given in Boynton, *et al.* (1966), and described formally in Pugh (1976) and Sigel and Pugh (1980). The essence of the field-additivity prediction is as follows. For the single class of photoreceptors mediating detection, quanta absorbed from a field of one wavelength (μ_1) are indistinguishable from an equal number of quanta absorbed from a field of a second wavelength (μ_2); and so, by equating the two fields for their threshold-elevating effect, we can equate them for the number of absorbed quanta. In other words, the hypotheses allow us to compute, for any monochromatic field, a value that is proportional to the number of absorbed quanta: this computed value is called the normalized field-intensity. Knowing the field sensitivities to each of the two fields in isolation, we can compute the normalized field-intensity for any mixture of the two fields. Knowing the relationship between the normalized field-intensity and threshold, we can specify exactly the threshfold-elevating effect of any mixture of the two fields.

Although logically our predictions depend on both Univariance and the field quantum-catch hypothesis, we view our experiments as tests of the latter, only. Should our experiments reject the conjunction of the two, we would not abandon Univariance, but rather the psychophysical linking hypothesis embodied in the field quantum-catch hypothesis.

In order to give the field quantum-catch hypothesis its best chance to obtain, our long-wavelength test was always 667 nm, fovealy presented, and 1° in diameter. The empirical results from this and the following paper can be summarized in two points.

(1) When we use a brief-duration (10 msec) test flash, we observe no significant deviations from either shape-invariance or field-additivity over backgrounds ranging in intensity from negligible to well into the bleaching range. That is, the data obtained with the brief flash are consistent with the field quantum-catch hypothesis.

(2) When we use a long-duration (200 msec) test flash, we confirm Stiles' (1953, 1959) findings of a dependence of the shape of the increment threshold upon the background wavelength. Stiles (1953) introduced the concept of a high-intensity mechanism, π_5', to describe these wavelength-dependent deviations from the standard shape increment-threshold curve. In the next paper we add the observation that the mixture of certain backgrounds, which in isolation each elevate the threshold more than 1 log unit, results in reliable violations of field-additivity. These violations yield the conclusion that the ability of the visual system to integrate increment-threshold signals over time from a single-wavelength test depends on the chromaticity of the adapting field.

This paper presents the results we obtained using a 10 msec test flash. The following paper contains the results obtained with a 200 msec flash. Based upon the pattern of results in both papers, we introduce two simple models of the visual pathways used for the detection of incremental signals originating in the long-wavelength cones..

METHODS

Optical apparatus

The light source was a high-pressure 75 W xenon arc (X-75, Illumination Industries) run under constant current. The light was stable to within less than 1% over any experimental session. Two beams were combined to form an 8° field in Maxwellian view. The third bean provided a 1° test target. Fiber optics attached to the test field stop provided orientation lights. Head alignment was maintained with a heavy-duty milling vice and bite-bar arrangement.

The test beam was rendered monochromatic by a concave grating monochromator (H-20, Jobin-Yvon) whose bandwidth was set to 2 nm. One of the field beans passed through an identical monochromator with bandwidth set to 8 nm. The second background bean was rendered monochromatic by blocked interference filters (Baird-Atomic, B16A, half-bandwidth 10 nm). Both background beams had neutral density wedges near focal points, so that the field intensities could be adjusted to the same level on different days, when desirable, despite small across-day variations in the light source.

A neutral density wedge was also mounted on a stepping motor at the exit slit of the test beam monochromator. Just past this position was a shutter (Uniblitz, 225L4A0X5, Vincent Associates).

Calibrations

Before each experimental session the radiant fluxes of the light beams were measured at the Maxwellian image. The measuring device was a silicon photodiode (Pin-10 DF, United Detector Technology) run in the photovoltaic (unbiased) mode. The voltage signal was amplified through a chopper-stabilized amplifier (Analog Devices 234J). The absolute calibration of the photodiode-amplifier was effected with an Eppley thermopile whose calibration had been verified by the manufacturer against an NBS standard.

The calibrations of the filters and monochromators have been described by Pugh (1976).

The shutter in the test beam generated a light pulse with a rise and fall time of about 2.5 msec. This was measured by running the photodiode in the fast (photoconductive) mode, and displaying the output directly on an oscilloscope.

Observers and procedures

The observers were one of the authors (Brian, 26

years old), and a paid undergraduate (Arnie, 22 years old). Both have normal color vision, as judged from standard tests.

The experiment was controlled by a computer. After adapting to the background field (minimum 30 sec at low intensities; minimum 2 min for backgrounds above 100 td) the observer signalled to the microprocessor, via a response box, that he was ready to begin the experiment. The threshold estimation procedure was a temporal, two-alternative, forced-choice staircase. Initially the test was set about 0.5 log units suprathreshold. Two computer-initiated tones defined temporal intervals separated by 1 sec. The observer had to choose the interval in which he thought the test had occurred. When the observer was right twice consecutively, the computer decremented the test intensity by 0.1 log units by means of the wedge mounted on the stepping motor in the test beam. Whenever an error was made the test intensity was incremented by 0.1 log units. After twelve reversals of direction the computer signalled an end to the staircase. The mean of the reversal densities was used as the estimate of the light intensity that yields a probability correct of 0.71 (Wetherhill, 1963). This intensity is taken to be the threshold. About 50–70 forced choice judgments, normally taking about 5–8 min, were required to obtain the requisite 12 reversals.

RESULTS

Shape-invariance and a 10 msec template

The Principle of Univariance, together with the field quantum-catch hypothesis, predict that the shape of the increment-threshold curve (plotted on log–log co-ordinates) must be independent of the field wavelength. In order to test this hypothesis, we first estimated a template based upon measurements from all of the increment-threshold data. We then compared the observations from each of the background wavelengths, singly, with this derived template. Shape-invariance is the prediction that the data from each background wavelength will follow the shape of the template derived from the pooled data.

Figures 1 and 2 (the lowest curves) show the results of pooling, in separate analyses, the data of 15 increment-threshold experiments for Brian, and 11 for Arnie. We have done this pooling by a computerized, iterative, least-squares fitting procedure (Sigel and Pugh, 1979). The plotted points in the lowest curve are the mean entries on the normalized field-intensity axis of the 0.10 log unit bins into which the data were pooled by the fitting procedure: the open and solid circles plot the means for bins that have been offset by 0.05 log units. Thus, each data point is averaged once into a bin represented by an open symbol, and once into a bin represented by a solid symbol. The smooth curve drawn through these solid and open symbols is the final, estimated template.

Figures 1 and 2 also give the complete results of the 26 increment-threshold experiments upon fields of five different wavelengths. The field wavelengths are the parameters labelling the curves. Each plotted symbol represents the threshold estimated from a staircase of 50–70 forced-choice trials, as described in Methods. Different symbols at each wavelength are the data of increment-threshold experiments executed on different days. The results for each successive field wavelength have been slid vertically 1/2 log unit above the curve just below it. Each set of points from the daily runs at each wavelength is placed in the position that minimizes its sum of squared deviations from the template. Table 1 gives the average absolute threshold, and the individual field points obtained from fitting the template to each increment-threshold curve.

There are two places in Figs 1 and 2 where some deviations from the template occur; (1) Arnie's 540 nm field data fall below the template at intensities that elevate the threshold less than 1 log unit. This is not true of Brian's data; (2) There is a tendency for threshold to rise above the template on 430 nm fields that elevate the threshold less than 1 log unit. For Brian's data in this region there are 9 above, 4 touching, and 4 below the template; for Arnie there are 7 above, 4 touching, and 4 below the template.

On the whole, the data collected on each of the various backgrounds follow quite well the template derived from the pooled data, and we thus do not reject shape-invariance. In Table 2 we give the numerical tabulation of the derived template. We shall show in the next paper that the same measurement techniques, used under exactly the same adapting conditions but with a different duration test flash, can reliably detect wavelength-dependent changes in the shape of the increment-threshold function.

Intermediate discussion

As can be seen from the data in Table 1, the sensitivity estimate for any single field wavelength varies across days. In general this variation is no more than about 0.15 log units from the across-day mean. Day-to-day variation of this magnitude occurs despite the fact that the daily estimates are based upon more than 500 forced-choice threshold observations.

An important implication of this variability is that our estimate of the field sensitivity of an observer from increment-threshold measurements made across only a few days is rather imprecise. Since the measurements we report here are based upon only three days, we cannot rule out the hypothesis that the variability of the field sensitivity is intrinsic to the observer, rather than mere measurement error. A lengthy, across-days experiment will be necessary to distinguish these hypotheses.

This variability also has important consequences for tests of the hypothesis that linear transformations of the π-mechanism field sensitivities can induce normal color matching functions. For, as Pugh and Sigel (1978) point out, variability as low as 0.01 log unit in estimates of the field sensitivities can have an enormous effect on the calculated unit coordinates. One

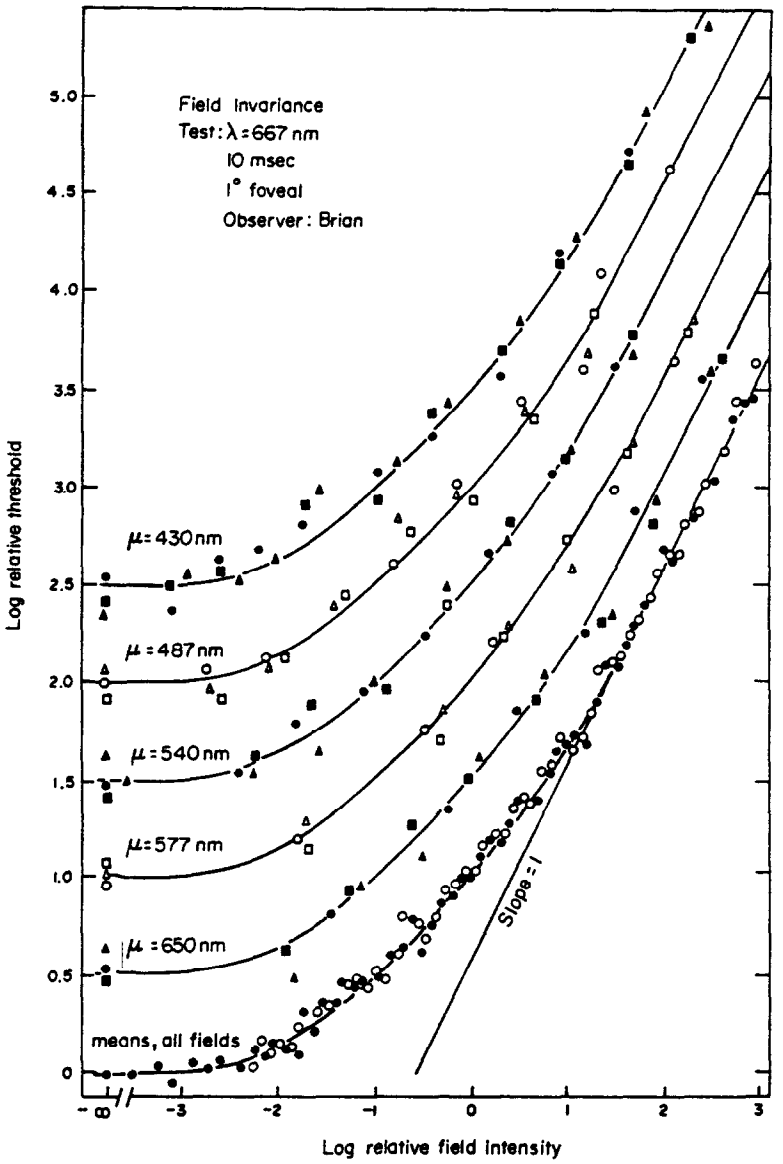

Fig. 1. Graph of threshold versus normalized field intensity for observer Brian. Each point in the upper portion of the graph is the threshold determined from 50–70 forced-choice trials, as described in Methods. The data are grouped by field wavelength. The lowermost curve gives the data pooled across all wavelengths; from these pooled data the template was derived, as described in the text. The template is shown as the smooth curve. This template was fit to each increment threshold curve separately to determine its position on the normalized field axis. The increment threshold graphs for each wavelength are displaced, vertically, by 1/2 log unit from the ones below it. See the text for a further description.

must interpret calculations from field sensitivity space to color-matching coordinates (e.g. Stiles, 1959; Estevez and Cavonius, 1978) with caution.

With the caveat about variability in mind, we present in Fig. 3 the field sensitivities one finds using the 10 msec test flash. The estimates for the two observers are plotted as open and solid symbols. The diamonds and triangles are the means (+2 SEM) obtained from fitting the 10 msec template to the full increment-threshold curves. The measurements represented by circles are not based on complete measurements of the increment-threshold curves. Rather, since we did not reject shape-invariance, we can assume that our 10 msec template in fact describes the shape of the increment-threshold curve for all background wavelengths when a 10 msec test flash is used. We measured increment-threshold on each of two background intensities (chosen so that threshold would be elevated approximately one log unit) for each wavelength at which a solid symbol is plotted. We fit the template through the absolute threshold and these two data points, using a least-squares criterion. The

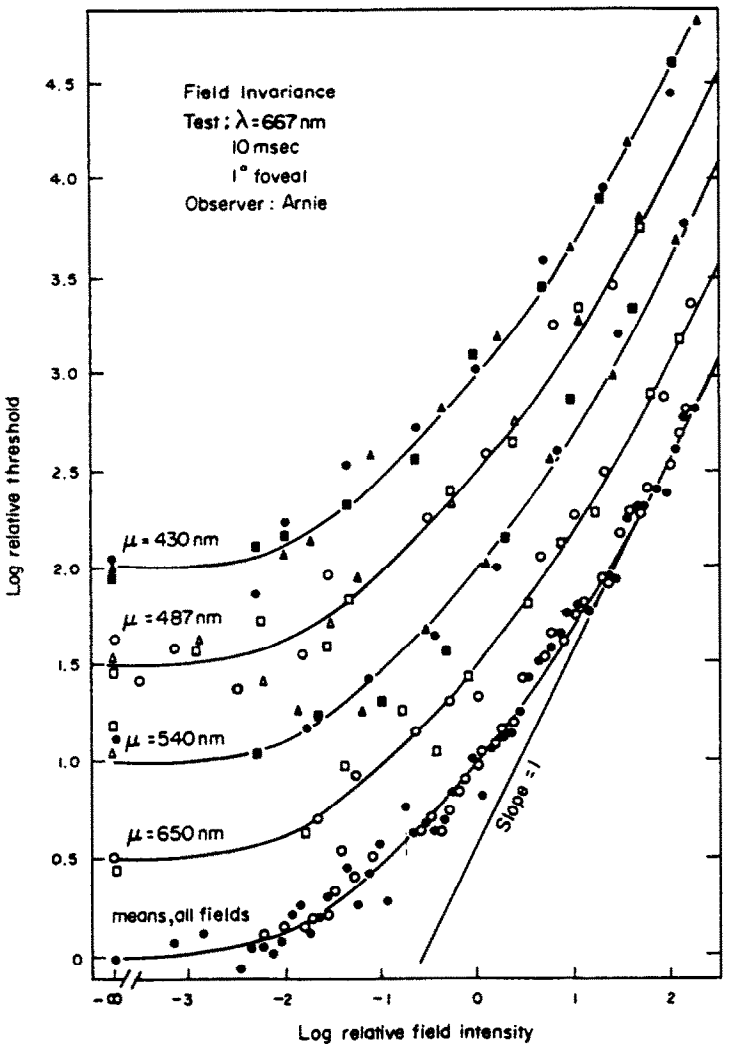

Fig. 2. Plot of threshold versus field intensity for observer Arnie. See caption of Fig. 1.

best-fitting position of the template determines the estimate of the field intensity required to elevate the threshold one log unit.

It is logically necessary for shape-invariance to hold before a field sensitivity can be defined. There is no *a priori* reason, however, that a field sensitivity should not depend on the parameters of the test light. Thus, the field sensitivity measured with a 10 msec test flash may well be different from that measured with a 200 msec, or any other, test probe. Nonetheless, the

Table 1. Field point* estimates

μ	From T.V.I. Curves	Mean ±2 SEM	From field-mixture experiments	Mean ±2 SEM
Observer: Brian; AVG. ABS. Threshold 7.00 ± 0.05 (N = 35)				
430	9.71, 9.53, 9.71	9.65 ± 0.12	9.42, 9.45, 9.55	9.48 ± 0.07
487	8.52, 8.51, 9.02	8.68 ± 0.34	8.58, 8.64, 8.66, 8.51	8.60 ± 0.07
540	8.16, 7.97, 7.46	8.03 ± 0.13	7.92, 7.43, 8.24, 8.33, 8.24	8.14 ± 0.18
577	8.03, 7.84, 7.91	7.93 ± 0.11	---	-
650	8.51, 8.23, 8.32	8.35 ± 0.17	8.45, 8.46, 8.51, 8.42, 8.36, 8.35, 8.40, 8.46	8.43 ± 0.05
Observer: Arnie; AVG. ABS. Threshold 7.55 ± 0.06 (N = 11)				
430	9.42, 9.17, 9.44	9.34 ± 0.18	9.11, 9.59, 9.59, 9.30, 9.22, 9.39	9.42 ± 0.15
487	9.16, 8.89, 8.92	8.99 ± 0.17	8.75, 8.75	8.75
540	8.12, 7.90, 8.36	8.13 ± 0.27	8.16, 8.21, 8.20, 8.30, 8.18, 8.14, 8.18, 8.18, 8.22	8.20 ± 0.03
650	8.77, 8.89 *	8.83 ± 0.10	8.76, 8.80, 8.73, 8.80, 8.58	8.74 ± 0.08

*The "field point" is the intensity of the field that causes a threshold deviation 1 log unit above absolute threshold. Units are log (quanta deg^{-2} sec^{-1}).

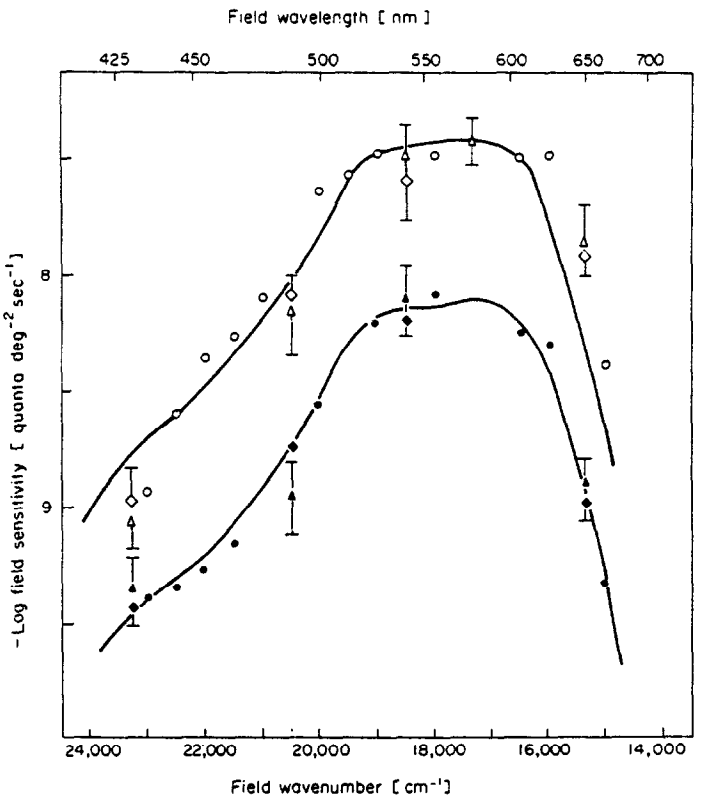

Fig. 3. The field sensitivity for observers Brian (open symbols) and Arnie (solid symbols). The open symbols are slid vertically by $\frac{1}{2}$ log unit. Circles are "three point" estimates as described in the text. The triangles and diamonds are estimates based on the full increment threshold measurements (triangles) and the field mixture measurements (diamonds). See Table 1 and the text for further description.

Table 2. Numerical tabulation* of 10 msec template

log x	log $\theta(x)$	log x	log $\theta(x)$
−3.0	0.000	−0.5	0.713
−2.9	0.008	−0.4	0.765
−2.8	0.015	−0.3	0.825
−2.7	0.027	−0.2	0.875
−2.6	0.028	−0.1	0.933
−2.5	0.037	0.0	1.000
−2.4	0.050	+0.1	1.052
−2.3	0.068	0.2	1.113
−2.2	0.085	0.3	1.175
−2.1	0.110	0.4	1.250
−2.0	0.126	0.5	1.310
−1.9	0.152	0.6	1.375
−1.8	0.188	0.7	1.445
−1.7	0.213	0.8	1.520
−1.6	0.250	0.9	1.588
−1.5	0.283	1.0	1.663
−1.4	0.325	1.1	1.735
−1.3	0.363	1.2	1.813
−1.2	0.396	1.3	1.900
−1.1	0.438	1.4	1.975
−1.0	0.475	1.5	2.062
−0.9	0.525	1.6	2.150
−0.8	0.575	—	—
−0.7	0.625	—	—
−0.6	0.670	—	—

* x is the normalized field-intensity coordinate; log $\theta(x)$ is the relative threshold elevation caused by a field of normalized intensity x.

field sensitivity of Stiles' long-wavelength mechanism, π_5, which was measured with a 200 msec test, is in good accord with the values we estimate in our experiments. This agreement is at first somewhat surprising in view of the fundamental differences in threshold behavior we show in the next paper for 200 msec increments. We shall argue (in the next paper), however, that the agreeement can be explained. In Fig. 3 we plot Stiles' average observer's π_5 field sensitivity along with our data. Arnie's function is very nearly that of the average observer. Brian's is broader (more sensitive) in the long-wavelength region of the spectrum.

Field-mixture experiments

Figure 4 shows the results of a field-mixture experiment for one observer, plotted in absolute physical units. These data were gathered within the span of a few days. This figure illustrates how the field-mixture experiments were executed.

The filled symbols show the average increment-threshold curves obtained with 650 nm and 540 nm fields, respectively. Rather than plot the individual runs as we have in Figs 1 and 2, we have averaged the results from the three days.

The intervening points were obtained in the field-mixture experiment proper. The leftmost point of each symbol type is the threshold on a 650 nm field at

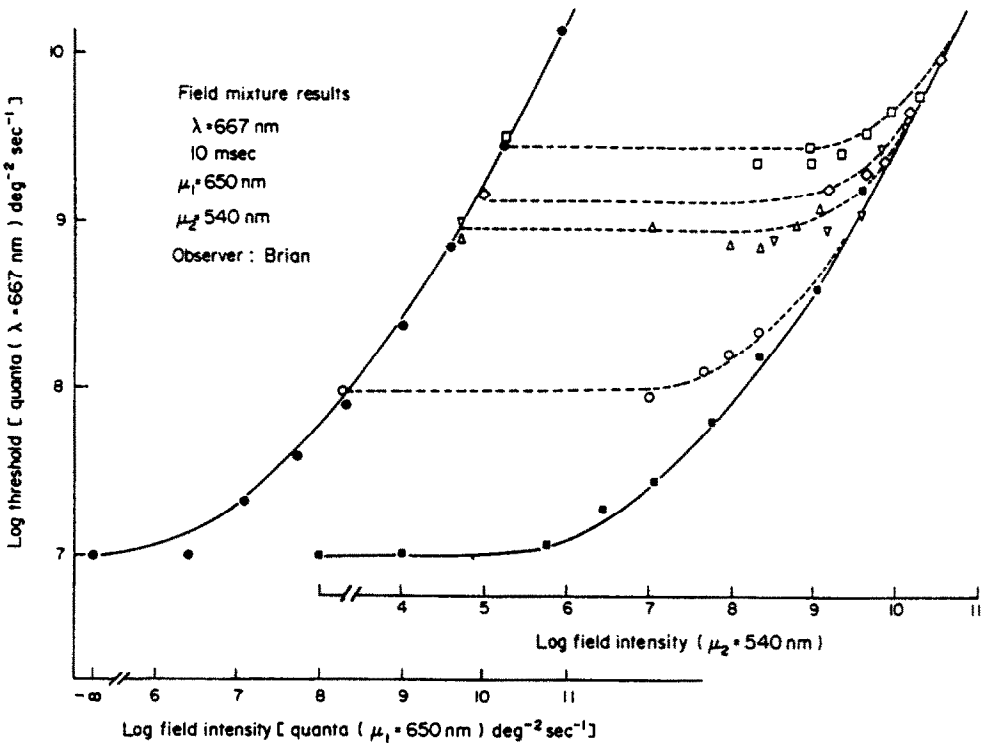

Fig. 4. A field-mixture experiment with 650 nm and 540 nm fields for observer Brian. The solid symbols are average increment-threshold curves, derived from the daily runs shown in Fig. 1. The intervening, open points are threshold measurements on a field mixture. The broken curves are the predictions of field additivity.

the intensity specified by the abscissa value. The other points with the same symbol, following the broken line across, were also measured with the same 650 nm field present, but with an admixed amount of a 540 nm field, specified by each point's position with respect to the 540 nm field-axis. The broken curves are the predictions of field-additivity.

These additivity predictions all have a common shape in log–log coordinates whenever both components of the field mixture are from an intensity region in which the threshold follows Weber's law, i.e. in which the slope of the increment-threshold curve is unity. In other words, the predicted shape of the graph of log threshold as a function of the intensity of the admixed field is always the same. Only the position of the predicted thresholds with respect to the two axes changes.

It is a simple algebraic manipulation to verify this assertion. We must show that if

$$\log \text{threshold} = \theta[\mu_1,\mu_2\ I_1,I_2]$$

is the dependence of log threshold upon the two field wavelengths and intensities, then for some constants, K_1, K_2, and function F,

$$\theta[\mu_1,\mu_2,I_1,I_2] = F[\log I_2 + K_2] + K_1 \qquad (1)$$

where K_1, K_2 are independent of $\log I_2$. In the region of Weber's law, we have, by field-additivity,

$$\theta[\mu_1,\mu_2,I_1,I_2] = log\,[\pi_{\mu_1} I_1 + \pi_{\mu_2} I_2]$$

where π_{μ_1}, π_{μ_2} are the field sensitivities at the two wavelengths μ_1 and μ_2. To see that this latter expression is of the same form as equation (1) simply make the following substitutions into equation (1): $K_1 = \log(\pi_{\mu_1} I_1)$; $K_2 = \log(\pi_{\mu_2}/\pi_{\mu_1} I_1)$; and $F(x) = \log[10^x + 1]$.

All of the field-mixture experiments we now report were executed upon fields from the Weber's law region. Therefore, we may summarize these mixture experiments by plotting the thresholds against a single common shape—the shape predicted by additivity. This is what we have done in Figs 5 and 6.

The data points in these two figures have been placed in the horizontal and vertical position that minimizes the total squared error from the additivity prediction. This position determines the values of the constants K_1 and K_2. Since I_1 is known, these constants provide independent estimates of the field sensitivity at those field wavelengths used in the mixture experiments. These estimates should be consistent with those obtained in the shape-invariance experiments. The values are given in Table 1.

There appear to be no systematic deviations from the additivity prediction in Figs 5 and 6. Table 1 confirms the consistency of the field sensitivity estimates from the mixture experiments with those from the

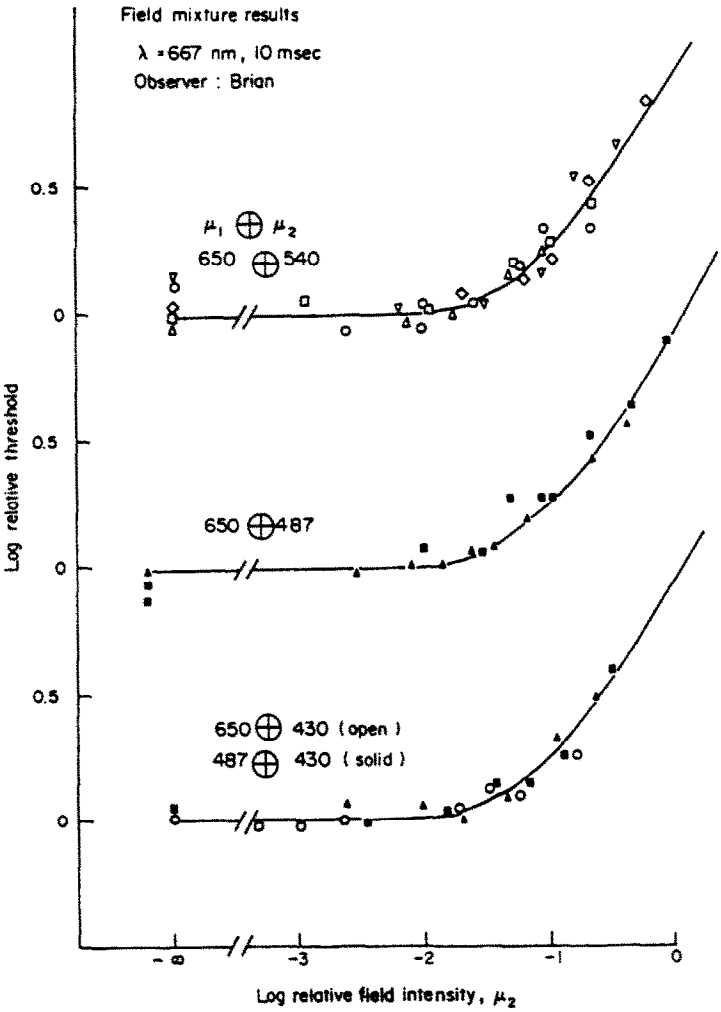

Fig. 5. A summary of the field-mixture studies with observer Brian. Each point is threshold determined from 50–70 forced-choice observations, as described in Methods. The different symbols refer to observations collected on different days. The data are grouped by field-mixture wavelengths. The smooth curve is the shape of the additivity prediction. See the text for a further description.

shape-invariance experiments. To further test the consistency of these results with the field quantum-catch hypothesis, we have performed a more detailed statistical analysis of the field-mixture data.

To subject the field quantum-catch hypothesis to a statistical test, one needs a reasonable alternative hypothesis. The alternative we have chosen is a class of functions that is consistent with the prediction of shape-invariance, but inconsistent with the prediction of field-additivity. This class of alternative functions is given in equation (2),

$$\log \text{threshold} = \log \zeta \left\{ \left[\sum_{i=1}^{3} (c_i q_i)^n \right]^{1/n} \right\} \qquad (2)$$

The q_i variables are the Vos and Walraven (1971) fundamentals; the c_i variables are free parameters. For the case $n = 1$, the spectral sensitivity of threshold elevation is a linear combination of the Vos and Walraven fundamentals (which, in turn, are a linear combination of the color matching functions). Therefore, when we test the (nested) hypothesis that $n = 1$, we are testing the hypothesis that the spectral sensitivity of threshold elevation in the field-additivity experiment is a linear combination of the cone spectral sensitivities. The alternative hypotheses, when n differs from one, may be thought of as perturbations about this hypothesis. It is only when $n = 1$ that the data are consistent with the field quantum-catch hypothesis. However, even if we do not reject the hypothesis that $n = 1$, hypotheses other than the field quantum-catch hypothesis remain possible. We pursue this issue further under the heading of Logical Implications and in the Appendix.

Computationally, the statistical test we performed was to determine how much the fit to the field-mixture data was improved when we let n vary freely, as compared with the best fit with n constrained to be one. It can be shown, under the assumption that log

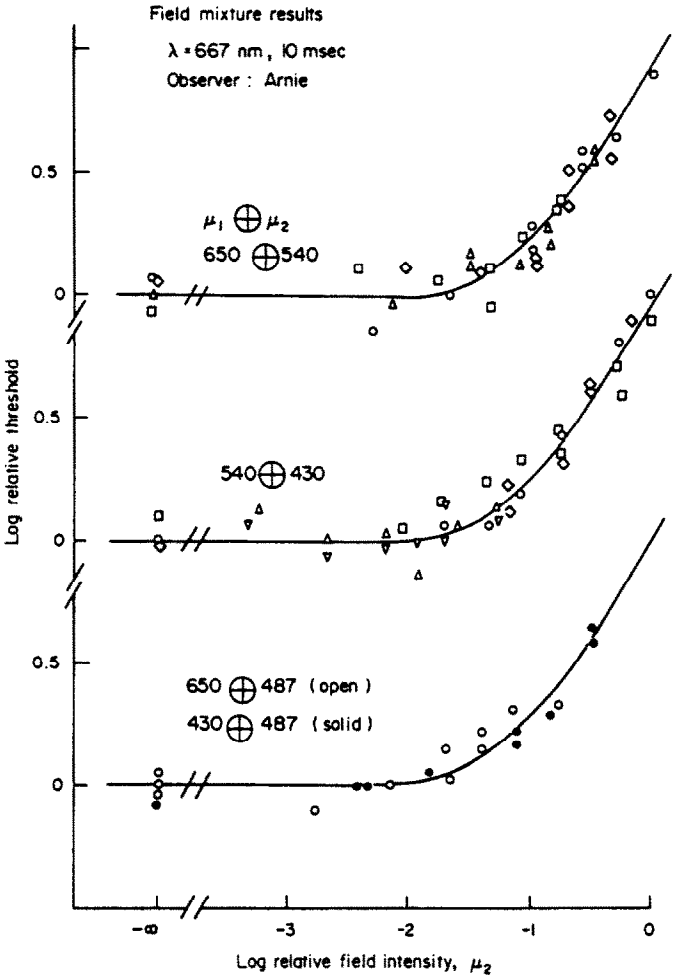

Fig. 6. A summary of the field mixture studies with observer Arnie. See the caption of Fig. 5.

threshold is approximately normally distributed, that

$$-2N \ln\left[\frac{\min(\text{MSE}, n = 1)}{\min(\text{MSE}, n \text{ free})}\right]$$

has a χ^2 distribution with one degree of freedom (Wilks, 1962), where N is the number of points to be fit, and MSE is the mean squared error. We fit the expression in equation (2) to each of the 19 sets of field-mixture data using an interative search procedure and least-squares criterion (Stepit, Chandler, 1965). We did this twice: once n was constrained to be equal to 1, and the second time n was varied to find the value that yielded the best fit. From the two fittings performed on each data set we obtained the χ^2 estimates for each set. Of the 19 sets of field-mixture data only two could reject the hypothesis that $n = 1$ at the 0.05 significance level. Therefore, this more formal statistical analysis yields a conclusion consonant with that of the analyses given above: these data do not reject the field quantum-catch hypothesis.

DISCUSSION

Empirical results

The increment-threshold data observed under the present testing conditions are in good accord with the shape-invariance and field-additivity properties. We shall predicate our discussion on the assumption that these properties are obeyed exactly.

Logical implications

Putting aside the statistical problems of hypothesis testing, we now take up the determination of the purely logical consequences that follow if one accepts the findings of shape-invariance and field-additivity. There seems to us to be only one plausible explanation for the shape-invariance and field-additivity properties: the field quantum-catch hypothesis is true, and the field sensitivity that we measure is that of the long-wavelength cones, as measured at the cornea.

The argument may be made informally as follows (we elaborate, with more formal analysis, in the Appendix). The rate of quantal absorption from a

field light for any class of cones is a linear function of the quantal flux at the cornea (excluding self-screening). Suppose now, contrary to the hypothesis that sensitivity depends only on the long-wavelength cones, that the field sensitivity depends upon more than one class of cones. These separate classes must communicate information about their individual quantum-catch rates to a common site where adaptation is controlled. Two possibilities exist. The first is that the steady-state signals which the cones signal to the common site are linear with the quantum catch of each, and that these are linearly combined at the common site. This final value then determines the state of adaptation. But the range over which the additivity predictions holds is many orders of magnitude. It seems most unlikely that steady-state photoreceptor signals remain linear over this entire range. Therefore, we reject the first possibility.

The second possibility is that the cones signal their steady-state quantum-catch rate nonlinearly. In this case the nonlinear input that is received at the common site must be inverted; these inverted values must then be summed in order to obtain a value to control the state of adaptation. Such a scheme of cancelling nonlinearities seems quite improbable. Therefore, we think that the most likely hypothesis is that the field sensitivity measured under the conditions we have used here is the spectral sensitivity of a single class of foveal cones.

We certainly do not conclude that all increment-thresholds—even all those measured with a deep red flash—are mediated by pathways that exhibit such simple adaptational control. Many experimenters have shown that both absolute and incremental detection depend, in some conditions, on the non-additive pooling of the signals of at least two classes of cones (e.g. Boynton *et al.*, 1964; Guth, 1965; Stiles, 1967). Indeed, Sternheim *et al.* (1979) have shown that field-sensitivity to low frequency, long-wavelength flickering increments is determined by signals from more than one class of cones.

The following paper reports increment-threshold measurements made with a 667 nm test flash of 200 msec. These measurements reject the field quantum-catch hypothesis, and thus yield the conclusion that this slight change in test parameter causes the detected signal to travel a pathway whose adaptation state depends on the quantum-catch rate of more than one class of cones.

Acknowledgements—This work was supported, in part, by NSF grant BNS 76-14192 to E. Pugh and NIH grant 1 ROI EY02164-01 to B. Wandell. We thank J. Larimer, J. Nachmias, and J. Thornton for their comments upon the manuscript. We also thank E. Adelson, L. Freedman, D. Hood and J. Yellott for useful discussions.

REFERENCES

Aczel J. (1966) *Lectures on Functional Equations and their Applications.* Academic Press, New York.

Boynton R. M., Ikeda M. and Stiles W. S. (1964) Interaction among chromatic mechanisms as inferred from positive and negative increment thresholds. *Vision Res.* **4**, 87–117.

Boynton R. M., Das S. R. and Gardiner J. (1966) Interactions among chromatic mechanisms revealed by mixing conditioning fields. *J. opt. Soc. Am.* **56**, 1775–1780.

Brindley G. S. (1957) Two theorems in colour vision. *Q. Jl exp. Psychol.* **9**, 101–104.

Brindley G. S. (1960) Two more visual theorems. *Q. Jl exp. Psychol.* **12**, 110–112.

Enoch J. M. (1972) The two-colour threshold technique of Stiles and derived component color mechanisms. In *Handbook of Sensory Physiology*, Vol. VII/4. Springer, Berlin.

Guth S. L. (1965) Luminance addition: general considerations and some results at foveal threshold. *J. opt. Soc. Am.* **55**, 718–722.

Helmholtz H. von (1896) *Handbuch der Physiologischen Optik*, 2nd edn. Voss, Hamburg.

Hurvich L. and Jameson D. (1955) Some quantitative aspects of an opponent-color theory. II. Brightness, saturation and hue in normal and dichromatic vision. *J. opt. Soc. Am.* **45**, 602–616.

Krantz D. H. (1975) Color measurement and color theory: representation theorem for Grassman structures. *J. math. Psychol.* **12**, 283–303.

Naka K. I. and Rushton W. A. H. (1966) An attempt to analyse colour reception by electrophysiology. *J. Physiol.* **185**, 587–599.

Pugh E. N. Jr (1976) The nature of the π_1 mechanism of W. S. Stiles. *J. Physiol.* **257**, 713–747.

Pugh E. N. Jr and Sigel C. A. (1978) Evaluation of the candidacy of the π-mechanisms of Stiles for color-matching fundamentals. *Vision Res.* **18**, 317–330.

Rodieck R. W. (1973) *The Vertebrate Retina.* Freeman, San Francisco.

Schroedinger E. (1920) Theorie de Pigmente von grossten Teuchtkraft. *Ann. Physik.* **62**, 603.

Sigel C. A. and Pugh E. N. Jr (1980) Stiles' π_5 color mechanism: Tests of field displacement and field additivity properties. *J. opt. Soc. Am.* **70**, 71–81.

Sirovich L. and Abramov I. (1977) Photopigments and pseudopigments. *Vision Res.* **17**, 5–16.

Sternheim C. E., Stromeyer C. F. and Khoo M. C. K. (1979) Visibility of chromatic flicker upon spectrally mixed adapting fields. *Vision Res.* **19**, 175–183.

Stiles W. S. (1939) The directional sensitivity of the retina and the spectral sensitivity of the rods and cones. *Proc. R. Soc.* **B127**, 64–105.

Stiles W. S. (1946) A modified Helmholtz line element in brightness-colour space. *Proc. phys. Soc.* **58**, 41–65.

Stiles W. S. (1953) Further studies of visual mechanisms by the two-colour threshold technique. *Colloq. sobre problems opticas de la vision*, Madrid. **1**, 65–103.

Stiles W. S. (1959) Color vision: the approach through increment threshold sensitivity. *Proc. natn. Acad. Sci.* **45**, 100–114.

Stiles W. S. (1967) Mechanism concepts in colour theory. *J. Colour Group No.* 11, 105–123.

Stiles W. S. (1978) *Mechanisms of Color Vision.* Academic Press, New York.

Vos J. J. and Walraven P. L. (1971) On the derivation of the foveal receptor primaries. *Vision Res.* **11**, 799–818.

Wetherhill G. B. (1963) Sequential estimation of quantal response curves. *Jl R. statist. Soc.* **B25**, 1–48.

Wilks S. S. (1962) *Mathematical Statistics.* Wiley, New York.

APPENDIX

This Appendix has three goals. The first is to show why shape invariance and field additivity, together, permit us to

conclude that the field sensitivity is a linear combination of the spectral sensitivities of the photopigments. The second goal is to argue that the field sensitivity is not an arbitrary linear functional of the photopigment sensitivities, but most likely it is proportional to the (uncorrected for media losses) sensitivity of the long-wavelength photopigment. The third is to motivate—from our theoretical treatment—the statistical analysis of our data that we described in the text.

The notation and logic we use here follows that of Krantz (1975). We denote field lights by lower-case italic letters from the beginning of the alphabet ($a, b, c, \ldots$). We introduce an operation, $*$, where $I*a$ is light a, adjusted in intensity by a real number, I. The symbol $*$ corresponds to the physical manipulation of inserting, or removing, a neutral density filter (of density $1/I$) from the path of light a. This changes the intensity of a but leaves its spectrum undisturbed. We also introduce the symbol $\oplus$ to denote the mixing of two fields, say, $a \oplus b$, by superimposing the two lights, a and b. Finally, we write

$$a \sim_{\pi_5} b$$

whenever threshold of the 667 nm, 10 msec test light is the same on field a as it is on field b. This expression is read as "a is π_5 equivalent to b". Empirically it means that a and b cause the threshold to be elevated by the same amount.

Notice that for any light, a, we can adjust the intensity of a standard light, s, by an amount $I(a)$ such that

$$a \sim_{\pi_5} I(a)*s.$$

That is, we can adjust the intensity of s such that threshold on the adjusted field, $I(a)*s$, equals threshold on a. Implicitly this function, $I(a)$, depends on the fact that we are equating for the π_5 mechanism. That is, given that the aforementioned adjustment is made, it will in general be false that $a \sim_{\pi_j} I(a)*s$, $j \neq 5$. Thus, when we write the function $I(a)$ it is more complete to write $I(a\pi_5)$. But because this notation is cumbersome and there is no ambiguity in what follows, we will suppress the second argument.

The field-additivity property, in general form may be written thus:

If

$$a \sim_{\pi_5} I(a)*s$$

and

$$b \sim_{\pi_5} I(b)*s \tag{1}$$

then

$$a \oplus b \sim_{\pi_5} [I(a) + I(b)]*s$$

Since by definition of $I(\cdot)$,

$$a \oplus b \sim_{\pi_5} I[a \oplus b]*s$$

testing property (1) is the same as testing

$$I(a \oplus b) = I(a) + I(b). \tag{2}$$

Notice that I is a function from the set of field lights into the real numbers. If (2) holds, I is a linear functional and therefore can be written as a weighted sum of the coordinates of a. In particular, we may represent lights by their quantum catches in the three cone types. Letting $a = (q_1(a), q_2(a), q_3(a))$ where $q_i(a)$ are the three quantum catches, we have from (2) that

$$I(a) = \sum_{i=1}^{3} \alpha_i q_i(a) \tag{3}$$

The usual means of evaluating the spectral sensitivity of π_5 is to measure the action spectrum of monochromatic field lights. Let 1_μ denote a monochromatic light of unit radiance and wavelength μ. The action spectrum of π_5 is found by adjusting the intensities of these lights by an amount $J(1_\mu)$ such that

$$J(1_\mu)*1_\mu \sim_{\pi_5} s$$

$J(1_\mu)$ is a field action spectrum of π_5 for standard s.

Since

$$1_\mu \sim_{\pi_5} I(1_\mu)*s$$

and it follows that

$$1/J[1_\mu] = I[1_\mu] = \sum_{i=1}^{3} \alpha_i q_i(1_\mu)$$

We therefore conclude that $I(1_\mu)$, which is proportional to the field sensitivity, is a linear combination of the cone spectral sensitivities.

II

We now argue that the most likely hypothesis is that the spectral sensitivity of π_5 is, in fact, that of the long wavelength cone itself. This argument is similar to the one made in Sigel and Pugh (1980).

Notice that threshold upon a field a can be written as depending only upon $I(a)$, since $I(a)$ is the scalar amount of the standard s that gives the same increment threshold. Thus,

$$\text{threshold} = \phi[I(a)],\ \phi \text{ monotone increasing.}$$

Suppose further that each class of cones contains a single pigment and that threshold depends upon the response of the three classes of cones via the function, P

$$\phi[I(a)] = P\{R_1[q_1(a)], R_2[q_2(a)], R_3[q_3(a)]\}.$$

We call P the "pooling function"; R_i are the response functions of the three cone types. Note that Univariance is implicit in this question since the R_i depend only on the respective quantum catches, q_i.

Since on the basis of field-additivity we have accepted equation (3), we have

$$\phi\left[\sum_{i=1}^{3} \alpha_i q_i(a)\right] = P\{R_1[q_1(a)],\ R_2[q_2(a)],\ R_3[q_3(a)]\}$$

If we let $R_i[q_i(a)] = x_i$, then

$$P(x_1, x_2, x_3) = \phi\left[\sum_{i=1}^{3} \alpha_i R_i^{-1}(x_i)\right] \tag{4}$$

That is, the pooling functions must be of the form given in (4).

There are two alternatives. Either the R_i are linear, or they are not. It is unlikely that the R_i remain linear over the many log units of quantum catch in these experiments. If we accept that they are non-linear, and that threshold depends upon more than one class of cones, we are forced by (4) to accept that the pooling function perfectly cancels the non-linearities of the cone outputs. Such cancelling non-linearities seem very implausible. Therefore, we take as the most likely hypothesis that

$$P(x_1, x_2, x_3) = f(x_1).$$

That is, threshold depends upon the quantum catch of a single class of cones.

III

Our arguments owe a large debt to the formulation of Krantz (1975) who extends and formalizes the discussion of Brindley (1957, 1960).

Another conceptually related paper is that of Sirovich and Abramov (1977). They begin their analysis at the pooling function which they write as

$$P\{R_1[q_1(a)],\ R_2[q_2(a)],\ R_3[q_3(a)]\} = F[q_1(a),\ q_2(a),\ q_3(a)].$$

They point out—as does Krantz (1975, p. 298)—that shape-invariance, without assuming additivity, implies the existence of a function, S, such that

$$F[q_1(N * a),\ q_2(N * a),\ q_3(N * a)] = H\{NS[q_1(a),\ q_2(a),\ q_3(a)]\} \quad (5)$$

where N is a scalar, and $q_i(N * a) = Nq_i(a)$, because (ignoring self-screening) quantum catch is a linear functional. Equation (5) implies

$$S[q_1(N * a),\ q_2(N * a),\ q_3(N * a)] = NS[q_1(a),\ q_2(a),\ q_3(a)]. \quad (6)$$

Thus, tests of shape-invariance may be thought of as tests of equation (6). The solution to equation (6) is (Aczel, 1965; Krantz, 1975)

$$S(x_1, x_2, x_3) = \left(\sum_{i=1}^{3} \beta_i x_i\right) \mathrm{T}[(x_2/x_1),\ (x_3/x_1)]$$

Sirovich and Abramov (1977) make the additional assumption that

$$\frac{\partial}{\partial N} S[Nx_1,\ Nx_2,\ Nx_3]^n|_{N=0} \quad (7)$$

exists for some $0 < n \leqslant 1$. We are, unfortunately, unaware of any empirical tests of this assumption. Sirovich and Abramov (1977) point out that equation (7) in the presence of equation (6) leads to the conclusion that

$$S(x_1, x_2, x_3) = \left(\sum_{i=1}^{3} (x_i^n)\right)^{1/n} \quad (8)$$

where n is the largest value in the half-open interval, (0, 1), which satisfies equation (7).

To summarize: empirical tests of shape-invariance are tests of the validity of equation (6). Empirical tests of additivity are tests of equation (8) for the case when $n = 1$. We know of no empirical tests for the intermediate case, represented by equations (7) or (8) when n is less than one. That is, we know of no empirical tests of the condition suggested by Sirovich and Abramov (1977). Nonetheless, equation (8) presents us with a concrete set of functions that are shape-invariant and yet non-additive. Because of their convenience, we used them in our statistical analysis as alternative hypotheses to the field quantum catch hypothesis. In this way we were able to evaluate the power of our empirical measurements.